Research

Special Issue – Causes and patterns of diversity in China

Multi-scale patterns of forest structure and species composition in relation to climate in northeast China

Jingyun Fang, Xiangping Wang, Yining Liu, Zhiyao Tang, Peter S. White and Nathan J. Sanders

J. Fang (jyfang@urban.pku.edu.cn), X. Wang, Y. Liu and Z. Tang, Dept of Ecology, College of Environmental Sciences, Key Laboratory of Earth Surface Processes of the Ministry of Education, Peking Univ., CN-100871 Beijing, PR China. JF also at: State Key Laboratory of Vegetation and Environmental Change, Inst. of Botany, Chinese Academy of Sciences, CN-100093 Beijing, PR China. XW also at: Key Laboratory of Silviculture and Conservation of the Ministry of Education, College of Forestry, Beijing Forestry Univ., CN-100083 Beijing, PR China. – P. S. White, Dept of Biology, Univ. of North Carolina, Chapel Hill, NC 27599-3280, USA. – N. J. Sanders, Dept of Ecology and Evolutionary Biology, Univ. of Tennessee, Knoxville, TN 37996, USA.

Though a number of studies have focused on the factors that shape the structure and dynamics of temperate forests, little is known about whether these factors vary with spatial scale. In this study we investigated compositional and structural patterns of forests across three spatial scales (plot, local assemblages and regions) in northeast China and asked whether climatic variables shape these patterns. Using a systematic sampling design, we measured diameter at breast height (DBH) and height of trees, and recorded the abundances, percent of cover and heights of shrubs and herbs in 141 plots from 10 nature reserves. We found that summer temperature accounted for most of the variation in species composition, both within and among forest types. DBH, tree height and total basal area all increased significantly with summer temperature while stem density decreased. The DBH frequency distribution depended strongly on temperature (especially winter temperature) and varied among spatial scales, and it tended to be more left-skewed as temperature increased. Taking together, our results suggest that a warming climate could lead to an increase in tree growth and the changes in size structure of temperate forests in northeast China. In particular, the proportion of large trees will in all likelihood increase while that of smaller trees will decrease. Shifts in forest structure in a warmed world will undoubtedly influence forest management practices, ecosystem dynamics, and species conservation.

The temperate forests of Europe, North America, and east Asia occupy more than ~25% of the forested area on the earth (Martin et al. 2001), holding ~20% of the total plant biomass, and ~10% of the terrestrial carbon (Bonan 2008, Pan et al. 2011). Thus, it is no surprise that numerous studies have sought to explain the structure and dynamics of these forests, and to examine their relationships with environmental factors. An emerging consensus suggests that the structure of temperate forests varies systematically with climatic conditions, both in east Asia and eastern North America (Terborgh 1985, Wang et al. 2006, 2009, Poulos and Camp 2010). Given that climate is changing, and forest structure might depend on climate, it is imperative to understand the factors that regulate forest structure in order to predict forest structure in the future.

Though temperate forests in Europe, North America, and Asia have similar structure and share close floristic affinity, forests in east Asia typically have the highest taxonomic diversity (White 1983, Huntley 1993, Latham and Ricklefs 1993). Forests in northeast (NE) China are particularly extensive (Grishin 1995, Zhou 1997, Xu 2001), with an area of 1.24×10^6 km², more than six times the size of England. The climate in northeast China is highly

variable, varying from warm temperate to cool temperate from south to north, and from humid to semi-arid from east to west. As a consequence, all three types of temperate forests that occur in east Asia (deciduous broadleaved forest, needle-leaved and broadleaved mixed forest, and cool–temperate needle-leaved forest) can be found in NE China (Zhou 1997, Zhang 2007). Due to this rich flora and fauna, this region has been designated as one of the 'hot spots' for biodiversity conservation in China (Chen 1998).

Although species composition and community structure of the temperate forests have been intensively studied at the plot level in NE China (Wang et al. 2006, 2009) as well as in other forests (Tyrrell and Crow 1994, Woods 2000a, b, Johnson et al. 2012), few studies have provided a comprehensive assessment for such an extensive area of temperate forests and explored the relationship between stand structure (especially DBH) and climatic factors, especially across broad spatial scales.

While it is widely recognized that distribution of forest and individual species are strongly affected by climate, whether and how the climate influences geographic patterns of forest structure remains an open question (Terborgh 1985, Aiba and Kitayama 1999, Enquist and Niklas 2001,

Quigley and Platt 2003). This is especially true for the size frequency distribution of trees within communities (i.e. DBH frequency distribution), and it is especially critical because the DBH frequency distribution links directly with forest production and dynamics, providing a basis for forest management and biodiversity conservation practices (Hutchings 1997, Enquist et al. 2009). Obtaining information on the DBH of individual trees among many sites, however, is highly labor intensive. As a result, the tree size distribution in relation to climate has seldom been quantified across extensive areas.

Using 141 plots sampled in 10 well-protected reserves across NE China, this study aims to 1) explore overall patterns of species composition and community structure for these temperate forests and compare the difference between primary and secondary forests, 2) quantify the DBH frequency distribution at plot, local and regional scales, and 3) examine whether climatic factors are related to the compositional and structural characteristics of the forests. The overarching purpose of this study is to assess if fundamental patterns of forest structure in NE China are likely to be sensitive to future climate change.

Material and methods

Obtaining the plot-level data and climate variables

We sampled 141 plots in ten protected nature reserves in NE China (Table 1, Supplementary material Appendix 1, Fig. A1), using a systematic sampling design. The plots were located in diverse geographic locations (between 41–52°N, 121.5–129°E) and varied in elevation from 350 to 2000 m a.s.l. The mean annual temperature in the plots ranged from −10.0 to 5.1°C, and annual precipitation from 470 to 1130 mm.

In each of the 141 plots (20 × 30 m), we measured DBH of all stems with a DBH ≥ 3 cm, and tree height for most stems (ca 70%). For shrubs (including trees with DBH < 3 cm) and herbs, we recorded the identities of species and their abundances, percent coverage and mean

height of the individuals of that species in each plot. For a detailed description of how the data were collected in each plot, see Fang et al. 2012.

We estimated monthly mean temperature and precipitation for each plots, using the geographic element method (Fang 1992, Wang et al. 2006) as shown in Eq. (1).

$$T \text{ (or } P) = a + b \text{ Latitude} + c \text{ Longitude} + d \text{ Altitude} \quad (1)$$

where T (or P) is monthly mean temperature (or precipitation), and a, b, c, and d are constants.

The model was obtained for each month using climatic data from 130 meteorological stations across NE China. A test of the models using independent data suggested that the predicted values obtained from this model were close to actually recorded temperatures, with an R^2 of 0.83 and 0.74 and a regression slope of 0.96 and 1.05 for mean annual temperature and precipitation, respectively (Wang et al. 2008).

We then calculated three climatic indices using the estimated monthly mean temperature and precipitation: 1) annual precipitation (AP, mm), as an estimate of water availability; 2) mean temperature for the coldest month (MTCM, °C), as a surrogate of absolute minimum temperature (Prentice et al. 1992); and 3) warmth index (WI, °C·month) (Kira 1945), as a growing season heat sum, which is calculated as $\sum(t_i - 5)$ (where t_i is monthly mean temperature > 5°C). For the details on these climatic indices, consult Fang and Lechowicz (2006).

Classification and ordination

Plots were classified into forest types with agglomerative cluster analysis, using the flexible beta method as a group linkage method, and Bray–Curtis dissimilarity as a distance measure. The cluster analysis was performed with a plot × species matrix using basal area of each tree species in each plot. We used non-metric multi-dimensional scaling (NMS) for the ordination of plots. NMS is one of the most robust methods for multi-variate data reduction, which is

Table 1. Information on geography, climate and vegetation for 10 study sites in northeast China. AMT = annual mean temperature, AP = annual precipitation. ‡Main forest types for different sites are: 1 = *Betula ermanii* forest (1300–1400 m a.s.l.), and *Larix gmelini* forest (< 1300 m a.s.l.) (Zhou 1997), 2 = *L. gmelini* forest (Zhao et al. 2004a), 3 = *L. gmelini* forest (observed in this study), 4 = *L. gmelini* forest (Wang et al. 2009), 5 = *Pinus koraiensis* forest (Zhou 1997), 6 = *Pinus koraiensis* forest, and secondary broadleaved mixed forest, 7 = secondary broadleaved mixed forest, 8 = *B. ermanii* forest (> 1500 m a.s.l.), *Picea jezoensis* and *Abies nephrolepis* forest (900–1100 m a.s.l.), *Pinus koraiensis*-broadleaved mixed forest and secondary broadleaved mixed forest (< 900 m a.s.l.), 9 = *B. ermanii* forest (1700–2000 m a.s.l.), *Picea jezoensis* and *A. nephrolepis* forest (1100–1700 m a.s.l.), *Pinus koraiensis*-broadleaved mixed forest (< 1100 m a.s.l.), and secondary broadleaved mixed forest (< 550 m a.s.l.) (Wang et al. 1980), 10 = subalpine forest, *Pinus koraiensis*-broadleaved mixed forest, and secondary broadleaved mixed forest.

Site	Latitude (°N)	Longitude (°E)	Altitude (m)	AMT (°C)	AP (mm)	Vegetation type‡
Mt Daxue	51°51′	122°02′	900~1530	−4.8	470	1
Mt Baikalu	51°37′	123°04′	450~1460	−5.6~−1.2	360~500	2
Mt Dabai	51°36′	123°31′	650~1500	−4.3	498	3
Genhe	50°49′~50°51′	121°30′~121°31′	780~1142	−5.4	450~550	4
Liangshui	47°07′~47°14′	128°48′~128°56′	280~707	−0.3	680	5
Langxiang	46°58′	128°47′	200~970	1.0	610	6
Mt Mao'er	45°20′~45°25′	127°30′~127°34′	300~805	2.8	724	7
Mt Datudingzi	44°24′	128°12′	350~1669	2.0~4.0	550~650	8
Mt Changbai	41°23′~42°36′	126°55′~129°00′	500~2691	−7.3~4.9	600~1340	9
Mt Laotudingzi	41°11′~41°22′	124°41′~125°05′	470–1325	6.3	870~1060	10

based on ranked distances and well suited to the non-normal data of community ecology (McCune and Mefford 1999). In our analyses, we conducted the NMS with a plot-species matrix using data of the relative basal area (RBA) of trees. PC-ORD 4.0 (McCune and Mefford 1999) was used for the classification and ordination analysis.

Similarity in species composition between and within forest types

We used the 'Analysis of Similarities' proposed by Clarke (1993) to examine the difference in species composition both between- and within-forest types, using the 'vegan' package of R 2.10 (R Development Core Team). As a non-parametric version of analysis of variance, the index is based on the rank order of dissimilarity values (Bray–Curtis dissimilarity was used in this study), as shown in Eq. (2).

$$R_B = \frac{4 \times (r_B - r_W)}{N(N-1)} \tag{2}$$

where R_B is the index of compositional difference between forest types, r_B and r_W are respectively the mean rank of dissimilarities of the between- and within-forest type, and N is the number of plots. The statistical significance of R_B is assessed by a permutation test (999 permutations; Clarke 1993).

The analysis of similarities was conducted for trees using relative basal area (RBA) data, and for the shrub and herb layers using relative abundance data. To measure the compositional difference between each pair of forest types, we calculated R_B using the plot × species matrix for all plots from two forest types (Supplementary material Appendix 1, Table A1). To measure the compositional difference among plots within a forest type, we used a plot × species matrix for all plots from that forest type to calculate the mean rank of dissimilarities (r_W).

We then examined how R_B and r_W were related to climate and other factors using general linear models (GLMs). For the within-forest difference in species composition, we used the averaged value of each climatic index and the successional stage (primary or secondary forest) for each forest type to explain r_W. For the between-forest compositional difference, we used the between-forest difference in climatic indices and combination of successional stages (primary vs primary forest, primary vs secondary forest, and secondary vs secondary forest), to explain R_B (Supplementary material Appendix 1, Table A1). To examine whether the compositional difference in tree layers affects the differences in composition of shrub and herb layers, we used the R_B values from the tree layer to explain shrub layer R_B, and used R_B values of tree and shrub layers to explain herb layer R_B in GLMs. In these analyses, climatic variables were first submitted to a stepwise selection to drop non-significant variables before building the final GLMs. Because dissimilarity data are inherently not independent, we did not test the significance of the explanatory terms with commonly used F-test. Instead, we assessed the significance with permutation tests in the lmPerm package of R 2.10.

Forest size structure

We examined the relationship between DBH (D, cm) and tree height (H, m) with a generalized allometric equation (Ogawa 1969, Sumida et al. 1997):

$$\frac{1}{H} = \frac{1}{aD^b} + \frac{1}{H^*} \tag{3}$$

where a, b and H* are the regression coefficients, and the biological meaning of H* is the estimated asymptote of tree height. Tree heights of individuals that were not measured in situ were estimated using Eq. (3), which was fit for each forest type by each site (Wang et al. 2006). The R^2 value of all equations used to estimate tree height was higher than 0.7 (most > 0.8).

DBH frequency distribution was fit by a power law function (Eq. 4):

$$f(D) = c \, D^\lambda \tag{4}$$

where f(D) is the DBH probability distribution, and c and λ are constants.

The power law function is widely used to describe size frequency distribution in forests and other ecosystems (Coomes et al. 2003, Muller-Landau et al. 2006, White et al. 2008). In this study we also used this function to fit the DBH frequency distribution. The binning-based method (binning trees into different DBH classes) is usually used to estimate the exponent (λ) in Eq. (4), but the result may be biased in plots with a small sample size; it is also influenced by the bin widths used (White et al. 2007, Stegen and White 2008, White et al. 2008). We therefore used the maximum likelihood method to estimate the λ value, which outperforms other methods in both accuracy and precision and has been widely applied in recent studies (White et al. 2008, Enquist et al. 2009). Skewness is another measure to quantify tree size asymmetry and commonly used in ecological studies (Hutchings 1997, Aiba and Kitayama 1999, Takahashi et al. 2001). In order to examine whether the DBH frequency distribution differed across spatial scales, we estimated the λ value and the skewness of the DBH frequency distribution at three scales: plot scale (each single plot), local scale (we pooled all plots within a forest type in a site together, and pooled all plots across all forest types in a site together), and regional scale (we pooled together all plots across sites for each forest type, and pooled all the plots across forest types and sites in this study). In addition, we related DBH skewness and λ values to climatic variables to examine the changes in DBH frequency distribution along climatic gradients.

Results

Forest types and plot ordination

The 141 plots sampled in this study were classified into nine forest types using the agglomerative cluster analysis: 1) *Betula ermanii* forest, 2) *Larix gmelini* forest, 3) *L. olgensis* forest, 4) *Picea jezoensis* and *Abies nephrolepis* forest, 5) *Pinus koraiensis* forest, 6) *P. koraiensis* and

deciduous broadleaved mixed forest, 7) *B. platyphylla* and *Populus davidiana* forest, 8) *Quercus mongolica* forest, and 9) deciduous broadleaved mixed forest (Supplementary material Appendix 1, Table A2, Fig. A2).

These nine forest types can be further categorized into three forest groups: subalpine/ subartic boreal forests (types 1–4), temperate needle–leaf and broadleaved mixed forests (types 5 and 6), and temperate deciduous broadleaved forests (types 7–9), which correspond well with the empirical vegetation classification in China (Zhou 1997, Zhang 2007).

Further, the NMS ordination showed that the distributions of these forest plots were closely related to both temperature and precipitation variables (Fig. 1). Axis 1 represents the gradient of summer warmth (WI, r = 0.83), while axis 2 depicts the gradients of annual precipitation (AP, r = −0.63) and winter coldness (MTCM, r = 0.59). As illustrated in Fig. 1, *L. gmelini* forests occurred in cold and relatively arid climates in northwest part of NE China, whilst in its humid eastern part, boreal forests (*B. ermanii* forest, *L. olgensis* forest, *P. jezoensis*, and *A. nephrolepis* forest) were replaced by other temperate forests, as summer temperature increased.

Species composition and its correlation with climate

The analysis of species similarities showed that species composition differed significantly among the forest types (Supplementary material Appendix 1, Table A1). The between-forest compositional difference (R_B) increased significantly with the climatic difference, but varied among forest layers (Fig. 2a–c, Table 2). The R_B for the herbaceous
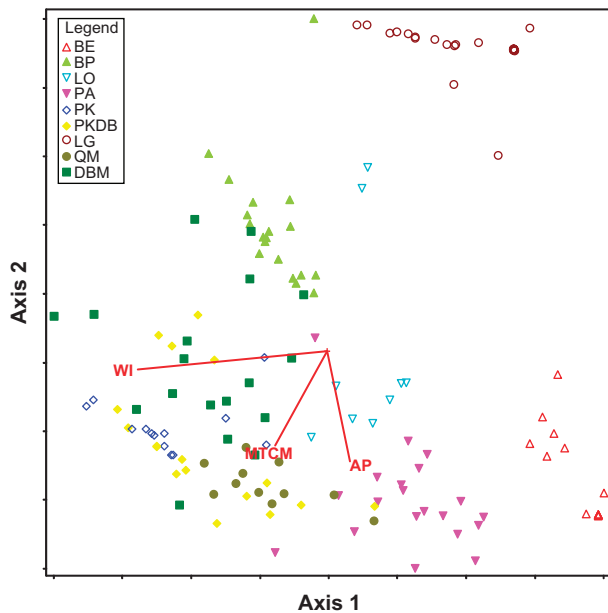

Figure 1. NMS biplots showing the relationship between forest composition and climatic indices. Abbreviations: BE = *Betula ermanii* forest, BP = *B. platyphylla* and *Populus davidiana* forest, LO = *Larix olgensis* forest, PA = *Picea jezoensis* and *A. nephrolepis* forest, PK = *Pinus koraiensis* forest, PKDB = *Pinus koraiensis* and deciduous broadleaved mixed forest, LG = *L. gmelini* forest, QM = *Q. mongolica* forest, DBM = deciduous broadleaved mixed forest.

layer was closely related to the R_B of the shrub layer (Fig. 2d), while the tree layer R_B was only weakly coupled to the R_B of herbs and shrubs ($R^2 < 0.2$, details not shown). Differences in climate between two plots explained 28.8% of variation in R_B values for the tree layer, but the explanatory power was higher for both the shrub layer (68.7%) and the herb layer (55.8%) (Table 2). Among the climatic indices, differences in WI (WI_{dif}) were far more powerful in explaining R_B than were AP (AP_{Dif}) and winter coldness ($MTCM_{dif}$). Successional stage (Suc) did not show significant effects in explaining the R_B values, for each of the tree, shrub and herb layers. On the other hand, shrub layer R_B significantly influenced variation in herb layer R_B (6.8%, p < 0.05) in GLM.

The within-forest compositional difference (r_W) was also mainly associated with heat sum (WI), but not with successional stage, precipitation and winter coldness (Table 3). Interestingly, shrub layer r_W was negatively related to WI while that of tree and herb layers were positively associated with WI (Fig. 2e–g). A significant relationship existed between the r_w value of shrub and tree layers (Fig. 2h), but not between other layers, indicating much larger difference in the effects of the different forest layers on the within-forest r_W compared with on the between-forest R_B.

Forest structure

Mean stem density differed remarkably among forest types, varying from 762 stems ha⁻¹ (in *Pinus koraiensis* forests) to ∼1700 stems ha⁻¹ (*B. platyphylla* and *P. davidiana* forests). DBH was inversely correlated with stem density. The most dense forest type had the lowest mean DBH (12.9 cm), while *P. koraiensis* forest showed a large DBH, with a mean DBH of 23.4 cm and maximum DBH averaged 77.8 cm (Supplementary material Appendix 1, Table A3).

Mean tree height varied from 15.4 m in *L. olgensis* forests, to 8.8 m in *B. ermanii* forests. The maximum tree height of the two *P. koraiensis* forests and *L. olgensis* forest averaged ∼30 m, while that of *B. ermanii* forest was the lowest (14.4 m). All forests except *B. ermanii* forests had a maximum value for maximum tree height of > 30 m.

The largest total basal area of trees (TBA) occurred in *L. olgensis* forests (52.6 m² ha⁻¹) and *P. koraiensis* forests (50.8 m² ha⁻¹), while that in *P. koraiensis* and broadleaved mixed forests, *P. jezoensis* and *A. nephrolepis* forests, and *Q. mongolica* forests ranged between 32.7 and 39.0 m² ha⁻¹. Other forests had a smaller TBA between 23.1 and 27.2 m² ha⁻¹ (Supplementary material Appendix 1, Table A3). *Betula ermanii* forest had the lowest tree height, but a relatively large TBA.

A correlation analysis showed that the above-mentioned structural measurements of forests were more closely related to thermal indices (especially WI) than precipitation across NE China (Fig. 3, Table 4). This was true not only for primary forests, but also for some characteristics of secondary forests.

DBH frequency distribution

We estimated the exponent (λ) in Eq. (4) and the skewness of the DBH frequency curve to describe the DBH
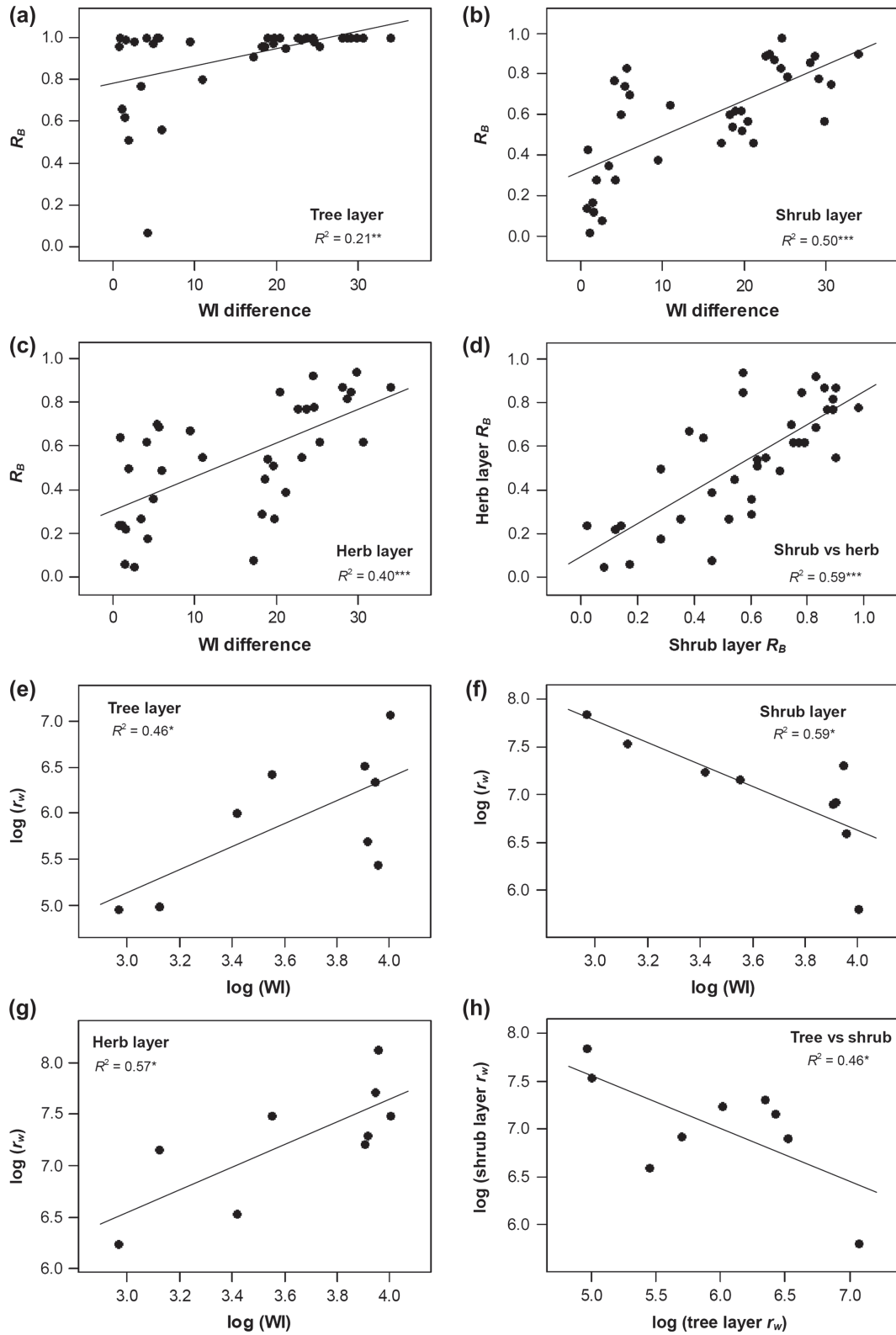
Figure 2. Between- and within-forest difference in species composition in relation to warmth index (WI) difference or WI (log-transformed) for nine forest types in NE China. Between-forest difference (a)–(d), i. e. R_B values in Supplementary material Appendix 1, Table A1, was plotted against the WI difference between each pair of forest types. (a) Tree layer, (b) shrub layer, (c) herb layer, and (d) R_B of shrub layer as a function to that of tree layer. The within-forest compositional difference (r_W, log transformed) (e)–(h) was plotted against log-transformed WI for (e) tree layer, (f) shrub layer, and (g) herb layer, (h) r_W of tree layer as a function to that of shrub layer.

Table 2. Effects of climate difference, successional stage (Suc) and upper-layer species composition on R_B values for tree, shrub and herb layers. Climatic indices used include the between-forest differences in warmth index (WI_{dif}), annual precipitation (AP_{dif}) and monthly mean temperature for the coldest month ($MTCM_{dif}$). These climatic variables were first applied to a stepwise regression to drop non-significant ones before they were included into the general linear models (GLMs). Successional stage was described by a category variable (Suc) including three categories: between primary forests, between secondary forests, and between primary and secondary forests. The degree of freedom (DF), mean squares (MS), and percentage of sum squares explained (%SS) are reported for each variable. Since R_B values were inherently not independent, the significances were not evaluated with F-test. Instead, the p-values obtained with permutation test are reported [p (perm)].

Layer and variable	DF	MS	p (perm)	%SS
Tree layer				
WI_{dif}	1	0.28	0.005	20.82
AP_{dif}	1	0.11	0.072	7.98
Suc	2	0.06	0.141	8.52
Residuals	31	0.03		62.68
Shrub layer				
WI_{dif}	1	1.25	0.001	49.92
AP_{dif}	1	0.37	0.001	14.58
$MTCM_{dif}$	1	0.10	0.058	4.16
Suc	2	0.00	0.883	0.17
Tree layer R_B	1	0.00	0.686	0.16
Residuals	29	0.03		31.01
Herb layer				
WI_{dif}	1	0.97	0.001	39.95
AP_{dif}	1	0.25	0.007	10.49
$MTCM_{dif}$	1	0.13	0.057	5.38
Suc	2	0.01	0.782	1.11
Tree layer R_B	1	0.00	0.980	0.01
Shrub layer R_B	1	0.16	0.030	6.82
Residuals	28	0.03		36.25

Table 3. Effects of climate and successional stage (Suc) and upper-layer species composition on within-forest difference (r_w, log transformed) in species composition for tree, shrub and herb layers. Climatic indices used include warmth index (WI), annual precipitation (AP) and monthly mean temperature for the coldest month (MTCM). However, AP and MTCM were excluded for the analysis during a stepwise regression. Successional stage was described with a category variable (Suc) including two categories, i.e. primary and secondary forests. The degree of freedom (DF), sum squares (SS), mean squares (MS), p-value of permutation test [p (perm)], and percentage of sum squares explained (%SS) were reported for each variable.

Layer and variable	DF	MS	p (perm)	SS%
Tree layer				
log(WI)	1	1.93	0.023	46.22
Suc	1	0.02	0.768	0.59
Residuals	6	0.37		53.19
Shrub layer				
log(WI)	1	1.64	0.013	59.17
Suc	1	0.06	0.584	2.32
Residuals	6	0.18		38.52
Herb layer				
log(WI)	1	1.50	0.024	57.21
Suc	1	0.21	0.300	7.90
Residuals	6	0.15		34.89

Discussion

Forest structure in relation to climate

Previous studies have suggested a close relationship between community structure and environmental factors in temperate forests (Terborgh 1985, Aiba and Kitayama 1999, Quigley and Platt 2003, Poulos and Camp 2010). However, most of these studies used indirect gradients (altitude and latitude) as a surrogate of climate. In our study, we used several different measures of contemporary climate, finding that climate does indeed influence the structure and dynamics of forests in NE China. Our results suggest that, given the importance of climate, ongoing climatic change has the potential to alter these forests in a number of different ways.

Our study showed that forest structural measurements were strongly correlated to climatic variables not only for primary forests, but also for some structural characteristics of secondary forests (Fig. 3, Table 4). Structural characteristics of the primary forests were closely correlated with temperature (WI, or winter temperature, MTCM); as temperature increased, stem density decreased, and other measurements (DBH, tree height and TBA) all increased. Compared with the primary forests, those in the secondary forests showed a large difference: at a similar condition of heat, the secondary forests had a lower DBH, tree height and TBA, but a higher stem density (Fig. 3).

These results suggest strong climatic control on regional patterns of forest structure, especially in the primary forests (Fig. 3). Among the climatic variables, temperature rather than precipitation was a major determinant of the structure of the primary forest (Table 4). These findings are similar to those from forests in humid mountains (Weaver and Murphy 1990, Pendry and Proctor 1997, Raich et al. 1997, Aiba and Kitayama 1999, Shen et al. 2004), suggesting that, regardless of system, temperature exerts strong effects on forest structures at regional scales.

frequency distribution across spatial scales. The λ value ranged between -2.68 and -1.46 with an average of -1.9 to -1.7 at the plot scale and between -2.43 and -1.62 at the local scale (Table 5). The value fell in a very narrow range of -1.96 to -1.66 for each forest type across the study region, with an overall value of -1.77 (Table 5, Fig. 4) (Supplementary material Appendix 1, Fig. A3 illustrates the details of the regional-scale DBH distribution for each forest type).

On the other hand, among the 141 plots, skewness of the DBH frequency distribution in 74 plots (52%) was ≥ 1.0. And in 42 plots (30%) skewness ranged between 0.5 and 1.0, and 24 plots (17%) between -0.5 and 0.5. Only one plot had a skewness value less than -0.5 (Fig. 4a). Skewness differed both between- and within-forest types; *B. ermanii* forest, *B. platyphylla* and *P. davidiana* forests, deciduous broadleaved mixed forest, and *L. olgensis* forest showed lower skewness, with a mean of < 0.9, while other forests had relatively higher skewness with a mean of > 1.0 (Fig. 4c). Skewness also differed among spatial scales (Table 5). For instance, at the plot-scale, the skewness for *B. ermanii* forests was between -0.01 and 1.57, with an average of 0.79, while at the local scale, it was 1.11 for Mt Changbai and 0.75 for Mt Datudingzi. The overall skewness at the regional scale, however, was 0.99. The λ value was related to DBH skewness at the plot and local scale (Fig. 4e) for both primary and secondary forests ($R^2 = 0.41$ and 0.29, respectively).
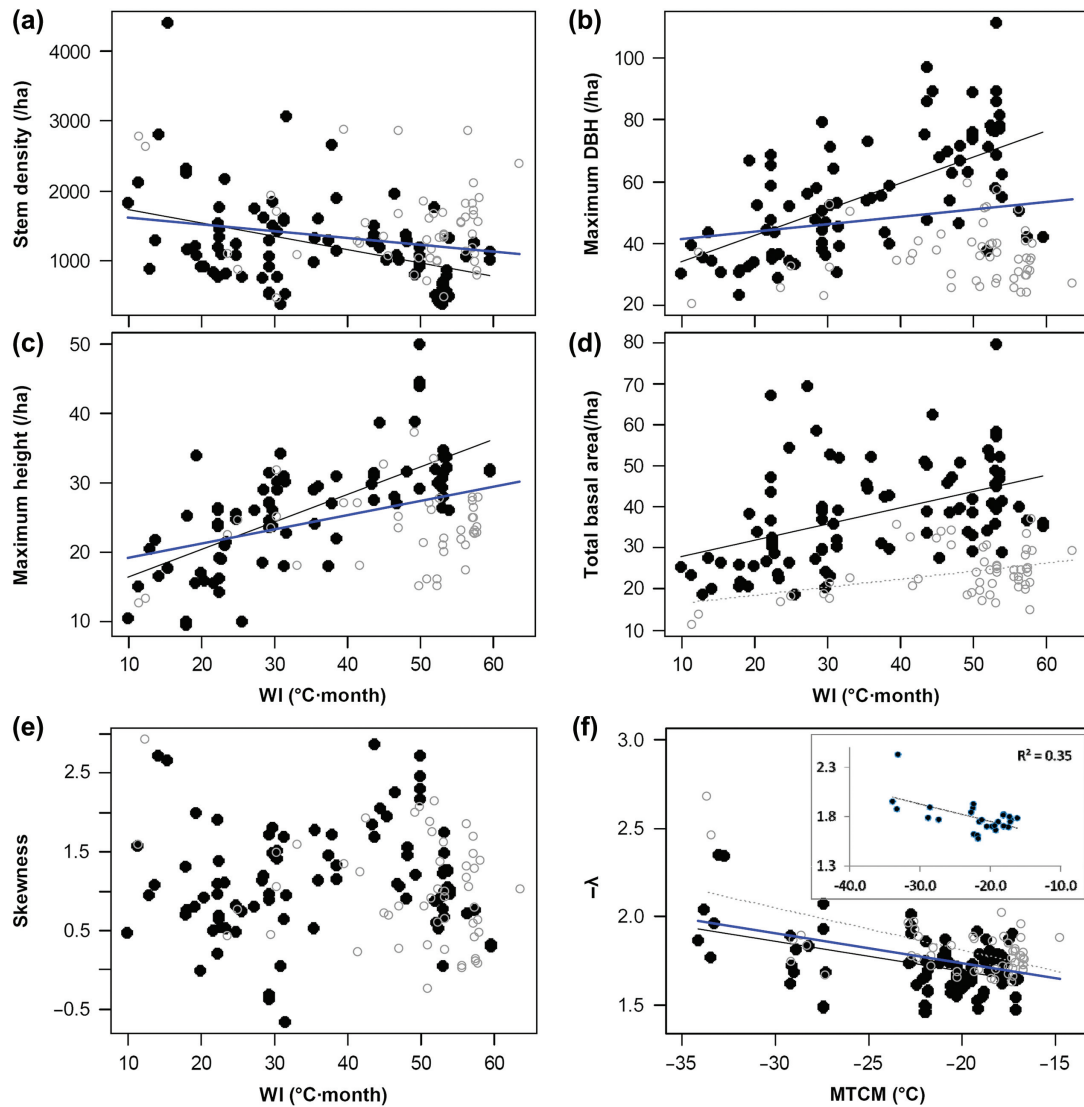
Figure 3. Relationships between structural characteristics and temperature (warmth index, WI; or mean temperature for the coldest month, MTCM) for each plot in NE China's forests. (a–d) stem density, maximum DBH, maximum height, and total basal area, respectively; (e) the skewness of DBH distribution frequency; (f) the $-\lambda$ value in the equation describing DBH frequency distribution ($f(D) = c\ D^\lambda$, see Methods). ● = primary forest (dark solid line); ○ = secondary forest (grey dotted line); blue bold line is the regression line for primary and secondary together. Regression line is plotted only for relationship with a significance level at $p < 0.05$. For R^2 and p-value of each regression, see Table 4. The subset figure in (f) showed the λ values for each forest type in a study site (i.e. the local scale in Table 5). Note that these λ values are not a mean of λ values calculated from each plot but were estimated by pooling all plots together in each forest type in a study site (see Methods).

Table 4. Correlations between measurements of forest structure and climatic indices for 141 plots across northeast China, and for primary and secondary forests separately. WI = warmth index, AP = annual precipitation, MTCM = monthly mean temperature for the coldest month, N = stem density, D_{mean} = mean DBH, D_{max} = maximum DBH, H_{mean} = mean tree height, H_{max} = maximum tree height, TBA = total basal area, Skewness = coefficient of skewness for DBHs in each plot, λ = the exponent in the power function for describing DBH frequency distribution: $f(D) = c\ D^\lambda$, ***$p < 0.001$, **$p < 0.01$, *$p < 0.05$, '$p < 0.1$ (2-tailed).

	Primary forests			Secondary forests			All together		
	WI	AP	MTCM	WI	AP	MTCM	WI	AP	MTCM
N (ha^{-1})	−0.41***	0.12	−0.25*	−0.16	0.13	−0.12	−0.22**	0.08	−0.16'
D_{mean} (cm)	0.41***	−0.03	0.32**	0.33*	0.2	0.41**	0.15'	0.1	0.2*
D_{max} (cm)	0.62***	−0.16	0.38***	0.07	0.15	0.12	0.18*	0.02	0.16'
H_{mean} (m)	0.44***	−0.18	0.29**	0.48***	0.15	0.51***	0.37***	−0.09	0.33***
H_{max} (m)	0.71***	−0.4***	0.27*	0.19	−0.22	0.07	0.42***	−0.28**	0.16'
TBA (m^2 ha^{-1})	0.45***	0.16	0.51***	0.39**	0.53***	0.57***	0.1	0.29***	0.3***
Skewness	0.1	−0.18'	−0.07	−0.27'	−0.01	−0.25'	−0.06	−0.11	−0.15'
λ	0.24*	0.26*	0.45***	0.54***	0.16	0.59***	0.2*	0.26**	0.43***

Some of our results are consistent with previous studies, but others are not. For instance, our results showing strong climatic control on tree height (Fig. 3c, Table 4) are consistent with those observed for more global analyses (Moles et al. 2009). The negative relationship between stem density and temperature is in line with that by Enquist and Niklas (2001), but contrasts with those of Quigley and Platt (2003) who did not find a significant relationship between stem density and temperature.

Changes in DBH frequency distribution with climate

The frequency distribution of DBH is one of key ways to describe a tree community (Tyrrell and Crow 1994, Woods 2000a). Thus, examining how it varies along climatic gradients is important for forest management practices in a changing climate (Peng et al. 2009). Previous studies in a variety of systems have investigated how environmental variables affect the size distribution of forests and suggested that skewness of the DBH distribution declined with increasing elevation in tropical montane systems (Aiba and Kitayama 1999), a reverse J-shaped tree height–size distribution in rain forests, and a unimodal distribution in boreal forests (Takahashi et al. 2001). Few studies, however, have reported the changes in the DBH distribution along extensive environmental gradients like the one we examine here (but see Condit et al. 1998). Our data demonstrate that skewness of DBH distribution was not related to contemporary climatic factors (Fig. 3e, Table 4). However, the changing rate ($-\lambda$ value in Eq. 4) of stem density vs DBH size significantly decreased with increasing temperature in both primary and secondary forests (Fig. 3f). This is true not only at the plot scale, but also at the local scale, suggesting that there may be a consistent climatic control of DBH distribution across spatial scales. Interestingly, while structural measurements, such as stem density, DBH and height, were more closely correlated with summer temperature (WI), the DBH distribution (λ value) was more closely related to winter coldness (MTCM) (Table 4).

A small changing rate ($-\lambda$ value in Eq. 4) of stem density against DBH size indicates a more left-skewed DBH distribution. This suggests that a warming climate could cause a more left skewed diameter distribution, namely the proportion of large trees would increase and that of small trees would decrease at a condition of increasing temperature, especially increasing winter temperature (Fig. 5). The schematic diagram in Fig. 5 has important implications for forest management and policy-making for adaptation of forestry to climate change.

DBH frequency distribution at different scales

The DBH frequency distribution gives insight into age structure, regeneration processes and stability of forest

Table 5. The λ value (exponent in Eq. 4) and skewness for DBH frequency distribution at different spatial scales. The λ values were estimated with maximum likelihood methods. At the regional scale, all plots within a forest type (or from all forest types) were pooled together to calculate the skewness and λ. For figures of DBH frequency distribution of each forest type, Supplementary material Appendix 1, Fig. A3. At the local scale, the λ value and skewness were calculated using all plots in a forest type in a study site, and for all plots in a study site. We also calculated the λ value and skewness for each plot, and their mean, maximum and minimum values were reported. Abbreviations for study sites: LTD = Mt Laotudingzi, CB = Mt Changbai, DTD = Mt Datudingzi, MRS = Mt Mao'er, LX = Langxiang Reserve, LS = Liangshui Reserve, GH = Genhe, DB = Mt Dabai, BKL = Mt Baikalu, DX = Mt Daxue. The nine forest types are: 1) BE = *Betula ermanii* forest, 2) LG = *Larix gmelini* forest, 3) LO = *L. olgensis* forest, 4) PA = *Picea jezoensis* and *Abies nephrolepis* forest, 5) PK = *Pinus koraiensis* forest, 6) PKDB = *Pinus koraiensis* and deciduous broadleaved mixed forest, 7) BP = *B. platyphylla* and *Populus davidiana* forest, 8) QM = *Quercus mongolica* forest, 9) DBM = deciduous broadleaved mixed forest.

| Forest type	Regional scale	Local scale										Plot scale		
		LTD	CB	DTD	MRS	LX	LS	GH	DBS	BKL	DXS	Mean	Max	Min
	λ value													
BE	−1.73	−	−1.70	−1.62	−	−	−	−	−	−	−1.95	−1.72	−1.57	−2.04
BP	−1.77	−	−1.76	−	−	−	−1.74	−	−	−1.89	−	−1.77	−1.64	−1.96
DBM	−1.77	−1.78	−1.74	−	−1.70	−1.88	−	−	−	−	−	−1.76	−1.62	−1.97
LG	−1.96	−	−	−	−	−	−	−1.77	−2.43	−1.79	−1.87	−1.90	−1.48	−2.68
LO	−1.66	−	−1.66	−	−	−	−	−	−	−	−	−1.62	−1.48	−1.92
PA	−1.73	−1.74	−1.70	−1.76	−	−	−	−	−	−	−	−1.73	−1.55	−1.89
PK	−1.68	−	−1.82	−	−	−	−1.61	−	−	−	−	−1.66	−1.46	−1.90
PKDB	−1.74	−1.70	−1.69	−	−	−1.84	−1.57	−	−	−	−	−1.73	−1.47	−2.02
QM	−1.82	−1.81	−1.79	−	−	−1.93	−	−	−	−	−	−1.80	−1.65	−2.02
All forest	−1.77	−1.78	−1.72	−1.75	−1.70	−1.87	−1.64	−1.77	−2.43	−1.80	−1.92	−1.76	−1.46	−2.68
	Skewness													
BE	0.99	−	1.11	0.75	−	−	−	−	−	−	1.05	0.79	1.57	−0.01
BP	1.11	−	1.15	−	−	−	0.01	−	−	0.44	−	0.88	1.84	0.02
DBM	1.04	1.40	0.62	−	0.40	2.37	−	−	−	−	−	0.79	2.07	−0.24
LG	1.91	−	−	−	−	−	−	1.05	2.80	1.99	1.03	1.27	2.92	−0.36
LO	1.04	−	1.04	−	−	−	−	−	−	−	−	0.69	1.84	−0.67
PA	1.75	1.64	1.69	1.74	−	−	−	−	−	−	−	1.39	2.86	0.21
PK	1.43	−	1.24	−	−	−	1.17	−	−	−	−	1.12	1.74	0.53
PKDB	2.01	0.93	1.84	−	−	2.59	1.03	−	−	−	−	1.57	2.87	0.05
QM	1.54	1.28	1.69	−	−	2.14	−	−	−	−	−	1.09	2.14	0.60
All forest	2.17	1.45	1.89	1.70	0.40	2.91	1.72	1.05	2.80	2.07	1.24	1.10	2.92	−0.67
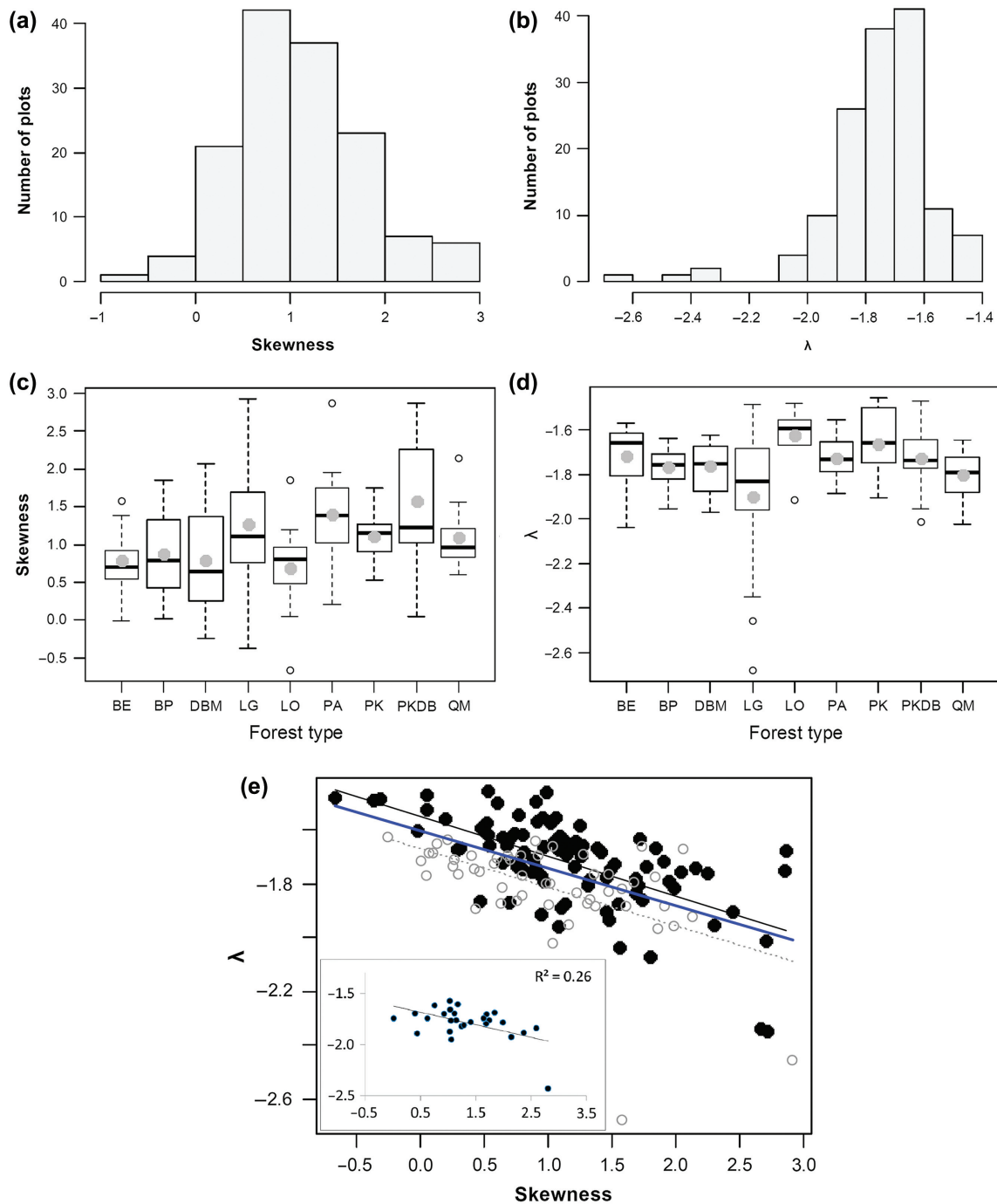
Figure 4. Skewness and λ (exponent in Eq. 4) of DBH size distribution for 141 plots in NE China. (a) Frequency distribution of skewness for all plots, (b) frequency distribution of λ values for all plots, (c) boxplot showing the skewness of each forest type, (d) λ values of each forest type, (e) relationship between λ values and skewness. ● = primary forests (dark solid line, $R^2 = 0.41$, $p < 0.001$); ○ = secondary forests (grey dotted line, $R^2 = 0.28$, $p < 0.001$); blue bold line is the regression line for primary and secondary together ($R^2 = 0.30$, $p < 0.001$). The subset figure shows the relationship between the λ value and skewness calculated for each forest type in a study site. Grey dots in (c) and (d) denote mean skewness or mean λ values. For abbreviations for each forest type, see Fig. 1.

communities (Mohler et al. 1978, Tyrrell and Crow 1994, Condit et al. 1998, Woods 2000a, b). Skewness is widely used to illustrate tree size asymmetry (Koyama and Kira 1956, Hutchings 1997, Takahashi et al. 2001). Our results showed that skewness is closely related to λ values (Fig. 4e), which supports the use of skewness as a measure in describing DBH frequency distribution. In general, the right-skewed

DBH frequency distribution suggests a continuously recruited and relatively stable community structure, while the left-skewed size distribution indicates a poor regeneration and more large individuals in the community. In this study, we found that skewness at the plot level differed remarkably among forest types (Table 5), but the overall (regional) DBH distribution of each forest type all showed
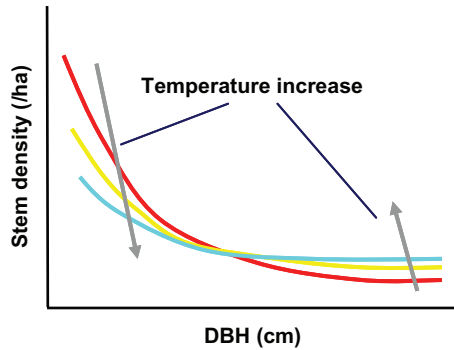
Figure 5. A scheme diagram for changes in stem density with DBH size under a condition of increasing temperature, derived from Fig. 3f. As temperature increases, DBH distribution frequency would be more left skewed, suggesting more large but less small trees.

a right-skewed pattern (skewness > 0.99; Table 5, Supplementary material Appendix 1, Fig. A3), suggesting that at the regional scale a continuous regeneration and stable age structure occur in most forest types in our study area.

Considering the scale-dependent diameter distribution as stated above, we propose the concept of multi-scale DBH frequency distribution, namely, plot, local and regional scale diameter frequency distribution, which have potential applications in forest management and conservation: 1) plot-scale diameter distribution: DBH distributions at the plot scale reflect the individual size distribution and regeneration characteristics within a patch (community). Most previous analyses on DBH frequency distribution were conducted at this scale (Tyrrell and Crow 1994, Aiba and Kitayama 1999, Woods 2000a, b, Takahashi et al. 2001); 2) local-scale diameter distribution: DBH distributions at local scales (or meta-community scale) reveal the overall regeneration dynamic for a forest type within a locality (such a mountain area as Mt Changbai in this study). A forest type will be stable at local scales if its overall DBH distribution indicates a continuous recruitment, although the DBH distributions of some patches (communities) may be left-skewed; and 3) regional-scale diameter distribution: regional DBH distributions can be used to evaluate the stability for a forest type in a region. Although some patches or localities may show a left-skewed frequency distribution, the forest type in this region could be stable in regeneration and age structure if its overall size distribution is right-skewed. Therefore, the regional DBH distribution may provide a useful tool for forest management and species conservation in the whole distribution range of the forest type.

Conclusions

Our results from local plots arrayed over an extensive environmental gradient indicate that contemporary climate – especially temperature – shapes the structure of temperate forests in NE China. Given that temperatures are projected to increase dramatically over the coming decades, understanding exactly how forests will respond to these changes will be a challenging, but vital task. Our analyses suggest that the proportion of large trees would increase and that of

small trees would decrease in the temperate forests in a warmed world. Based on an analysis on multi-scale size structure of forests, we propose the concept of multi-scale (plot, local and regional) DBH frequency distribution, which can have implications in regional forest management and species conservation, especially in a world where forests are confronted with ongoing climate change.

References

Aiba, S. I. and Kitayama, K. 1999. Structure, composition and species diversity in an altitude-substrate matrix of rain forest tree communities on Mount Kinabalu, Borneo. – Plant Ecol. 140: 139–157.

Bonan, G. B. et al. 2008. Forests and climate change: forcings, feedbacks, and the climate benefits of forests. – Science 320: 1444–1449.

Chen, C. D. (ed.) 1998. China's biodiversity: a country study organized by State Environmental Protection Administration. – China Environmental Science Press, Beijing.

Clarke, K. R. 1993. Non-parametric multivariate analysis of changes in community structure. – Aust. J. Ecol. 18: 117–143.

Condit, R. et al. 1998. Predicting population trends from size distribution: a direct test in a tropical tree community. – Am. Nat. 152: 495–509.

Coomes, D. A. et al. 2003. Disturbances prevent stem size-density distributions in natural forests from following scaling relationships. – Ecol. Lett. 6: 980–989.

Enquist, B. J. and Niklas, K. J. 2001. Invariant scaling relations across tree-dominated communities. – Nature 410: 655–660.

Enquist, B. J. et al. 2009. Extensions and evaluations of a general quantitative theory of forest structure and dynamics. – Proc. Natl Acad. Sci USA 106: 7046–7051.

Fang, J. Y. 1992. Study on the geographic elements affecting temperature distribution in China. – Acta Ecol. Sin. 12: 97–104.

Fang, J. Y. and Lechowicz, M. J. 2006. Climatic limits for the present distribution of beech (*Fagus* L.) species in the world. – J. Biogeogr. 33: 1804–1819.

Fang, J. et al. 2012. Forest community survey and the structural characteristics of forests in China. – Ecography 35: 1059–1071.

Grishin, S. Y. 1995. The boreal forests of north-eastern Eurasia. – Vegetatio 1995: 11–21.

Huntley, B. 1993. Species-richness in north–temperate zone forests. – J. Biogeogr. 20: 163–183.

Hutchings, M. J. 1997. The structure of plant populations. – In: Crawley, M. J. (ed.), Plant ecology. Blackwell, pp. 325–358.

Johnson, D. J. et al. 2012. Conspecific negative density dependence and forest diversity. – Science 336: 904–907.

Kira, T. 1945. A new classification of climate in eastern Asia as the basis for agricultural geography. – Horticult. Inst. Kyoto Univ.

Koyama, H. and Kira, T. 1956. Intraspecific competition among higher plants. VIII. Frequency distribution of individual plant weight as affected by the interaction between plants. – J. Inst. Polytech. Osaka City Univ. Ser. D 7: 73–94.

Latham, R. E. and Ricklefs, R. E. 1993. Global patterns of tree species richness in moist forests: energy diversity theory does not account for variation in species richness. – Oikos 67: 325–333.

Martin, P. H. et al. 2001. Carbon sinks in temperate forests. – Annu. Rev. Energy Environ. 26: 435–465.

McCune, B. and Mefford, M. J. 1999. PC-ORD. Multivariate analysis of ecological data, ver. 4. – MjM Software Design.

Mohler, C. L. et al. 1978. Stand structure and allometry of trees during self-thinning of pure stands. – J. Ecol. 66: 599–614.

Moles, A. T. et al. 2009. Global patterns in plant height. – J. Ecol. 97: 923–932.

Muller-Landau, H. C. et al. 2006. Comparing tropical forest tree size distributions with the predictions of metabolic ecology and equilibrium models. – Ecol. Lett. 9: 589–602.

Ogawa, H. 1969. An attempt at classifying forest types based on the relationship between tree height and d.b.h. – In: Kira, T. (ed.), Comparative study of primary productivity in forest ecosystems. JIBP-PT-F progress reports for 1968, pp. 3–17.

Pan, Y. D. et al. 2011. A large and persistent carbon sink in the world's forests. – Science 333: 988–993.

Pendry, C. A. and Proctor, J. 1997. Altitudinal zonation of rain forest on Bukit Belalong, Brunei: soils, forest structure and floristics. – J. Trop. Ecol. 13: 221–241.

Peng, C. et al. 2009. Quantifying the response of forest carbon balance to future climate change in northeastern China: model validation and prediction. – Global Planetary Change 66: 179–194.

Poulos, H. M. and Camp, A. E. 2010. Topographic influences on vegetation mosaics and tree diversity in the Chihuahuan Desert Borderlands. – Ecology 91: 1140–1151.

Prentice, I. C. et al. 1992. A global biome model based on plant physiology and dominance, soil properties and climate. – J. Biogeogr. 19: 117–134.

Quigley, M. F. and Platt, W. L. 2003. Composition and structure of seasonally deciduous forests in the Americas. – Ecol. Monogr. 73: 87–106.

Raich, J. W. et al. 1997. Primary productivity and ecosystem development along an elevational gradient on Mauna Loa, Hawaii. – Ecology 78: 707–721.

Shen, Z. H. et al. 2004. Altitudinal changes in species diversity and community structure of *Abies fabri* communities at Hailuo valley of Mt Gongga, Sichuna. – Biodivers. Sci. 12: 237–244.

Stegen, J. C. and White, E. P. 2008. On the relationship between mass and diameter distributions in tree communities. – Ecol. Lett. 11: 1287–1293.

Sumida, A. et al. 1997. Trade-off between height growth and stem diameter growth for an evergreen oak, *Quercus glauca*, in a mixed hardwood forest. – Funct. Ecol. 11: 300–309.

Takahashi, K. et al. 2001. Stand structure and regeneration in a Kamchatka mixed boreal forest. – J. Veg. Sci. 12: 627–634.

Terborgh, J. 1985. The vertical component of plant species diversity in temperate and tropical forests. – Am. Nat. 126: 760–776.

Tyrrell, L. E. and Crow, T. R. 1994. Structural characteristics of old-growth hemlock-hardwood forests in relation to age. – Ecology 75: 370–386.

Wang, X. P. et al. 2006. Climatic control on forests and tree species distribution in the forest region of northeast China. – J. Integrative Plant Biol. 48: 778–789.

Wang, X. P. et al. 2008. Forest biomass and root-shoot allocation in northeast China. – For. Ecol. Manage. 255: 4007–4020.

Wang, X. P. et al. 2009. Relative importance of climate vs local factors in shaping the regional patterns of forest plant richness across northeast China. – Ecography 32: 133–142.

Wang, Z. et al. 1980. The main forest types and their features of community structure in northern slope of Changbai Mountain (1). – Res. For. Ecosyst. 1: 25–42.

Weaver, P. L. and Murphy, P. G. 1990. Forest structure and productivity in Puerto Rico's Luquillo Mountains. – Biotropica 22: 69–82.

White, P. S. 1983. East Asian–east North American floristic relations: the plant community level. – Ann. Miss. Bot. Gard. 70: 734–747.

White, E. P. et al. 2007. Relationships between body size and abundance in ecology. –Trends Ecol. Evol. 22: 323–330.

White, E. P. et al. 2008. On estimating the exponent of power-law frequency distributions. – Ecology 89: 905–912.

Woods, K. D. 2000a. Long-term change and spatial pattern in a late-successional hemlock-northern hardwood forest. – J. Ecol. 88: 267–282.

Woods, K. D. 2000b. Dynamics in late-successional hemlock–hardwood forests over three decades. – Ecology 81: 110–126.

Xu, H. C. 2001. Natural forests of *Pinus koraiensis* in China. – China Forestry Publ. House, Beijing.

Zhang, X. S. (ed.) 2007. Vegetation of China and its geographic patterns. – China Geology Publ. House, Beijing.

Zhao, S. Q. et al. 2004. Structure and species diversity of boreal forests in Mt. Baikalu, Huzhong area, Daxing'an Mountains, northeast China. – Biodivers. Sci. 12: 182–189.

Zhou, Y. L. (ed.) 1997. Geography of the vegetation in northeast China. – Science Press, Beijing.

Supplementary material (Appendix ECOG-00086 at < www.oikosoffice.lu.se/appendix >). Appendix 1.